JACS
JOURNAL OF THE AMERICAN CHEMICAL SOCIETY
pubs.acs.org/JACS
Article

Anionic Lipids Regulate the Light-Harvesting Complex 1-Reaction Center Photocycle in Purple Bacteria

Olivia C. Fiebig, Graham P. Schmidt, Neetu Singh Yadav, Dihao Wang, Muath Nairat, Helen Tang, Yi Ji, Valérie Prima, James N. Sturgis, Josh V. Vermaas, Dvir Harris, and Gabriela S. Schlau-Cohen*

Cite This: J. Am. Chem. Soc. 2025, 147, 36706−36716
Read Online
ACCESS | Metrics & More | Article Recommendations | Supporting Information

ABSTRACT: Photosynthetic purple bacteria can capture and convert sunlight with a remarkable, nearly 100% quantum efficiency. The light-harvesting complex 1-reaction center (LH1-RC) core complex is the membrane complex fundamentally responsible for solar energy conversion. LH1-RC has a highly conserved surrounding lipid composition known to favor anionic lipids for an unknown function. In this work, we compared experimentally the rate of LH1-to-RC energy transfer in detergent, membrane nanodiscs with varying lipid compositions, purified membrane fragments, and live cells. The energy transfer rate indicated that RC turnover decreased in neutral lipids, yet was partially restored in anionic lipids, revealing an unexpected lipid dependence. In complementary molecular dynamics simulations, the anionic lipid cardiolipin showed electrostatic interactions with LH1-RC that may mediate quinone exchange, providing a mechanism for the observed lipid dependence. Overall, these results revealed that anionic lipids facilitate LH1-RC redox cycling, identifying a functional role for membrane composition in photosynthetic solar energy conversion.

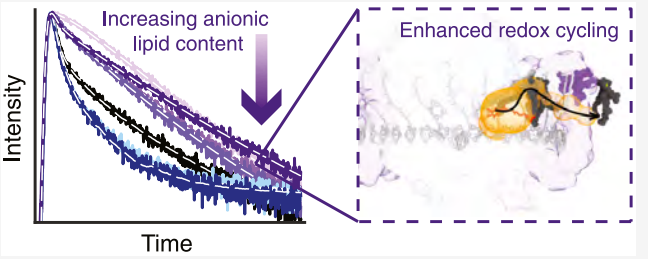

INTRODUCTION

Photosynthetic purple bacteria capture and convert sunlight with high quantum efficiency through a network of proteins in the intracytoplasmic membrane (ICM).[1] The most essential part of the purple bacterial photosynthetic machinery is the light-harvesting complex 1-reaction center (LH1-RC) core complex, which is conserved across all species.[2] LH1-RC translates absorbed photons into separated charges through a series of energy and charge transfer steps that have been well characterized over the past decades.[3] The surrounding ICM itself is an active and dynamic environment, containing a diverse set of lipids that are highly regulated in proportion and location depending on environmental conditions.[4−6] The rationale behind their bioregulation is not clear, in large part because the influence of these lipids on the functional processes of energy and charge transfer has not been investigated.

The cell membrane of purple bacteria contains primarily phospholipids.[6,7] Recent work has shown that the lipid bilayer can influence both the organization and excited-state dynamics of photosynthetic proteins.[8−11] The cell membrane typically contains the zwitterionic phosphatidylcholine (PC) and/or phosphatidylethanolamine (PE) headgroups as well as the anionic phosphatidylglycerol (PG) and cardiolipin (CL) headgroups. While the specific lipid composition and ratios can vary between species and with growth conditions,[5−7] the major phospholipids in *Roseobacter (Rsb.) denitrificans* are PC, PG, and CL,[12,13] which is a distribution of lipid charges consistent with other species.[6,7] Although anionic lipids generally make up only 33% of the ICM, studies have shown that the local lipid composition associated with the LH1-RC complex is primarily anionic, as the percentage jumps to 66% of lipids copurified with LH1-RC.[6] Even more dramatically, CL only makes up approximately 10% of the total photosynthetic membrane, yet it is the dominant lipid associated with purified LH1-RC.[6] Previous work has shown that the anionic PG and CL stabilize the charge-separated state in the reaction center and influence the quinone binding site through electrostatic interactions.[14−16] CL, in particular, has a unique structure, carrying both twice the charge (−2) and the number of acyl tails (4) as PG (Figure 1A). Studies of LH1-RC have found CL tightly bound to LH1-RC,[17] with preferential orientation on the cytoplasmic side of the membrane near the RC quinone binding sites.[18−20]

LH1-RC from *Rsb. denitrificans* consists of a ring-shaped antenna, LH1, that surrounds the RC. LH1 contains 14−16 protein subunits that each bind two bacteriochlorophyll a

Received: July 18, 2025
Revised: September 1, 2025
Accepted: September 2, 2025
Published: September 23, 2025

https://doi.org/10.1021/jacs.5c12301
J. Am. Chem. Soc. 2025, 147, 36706−36716

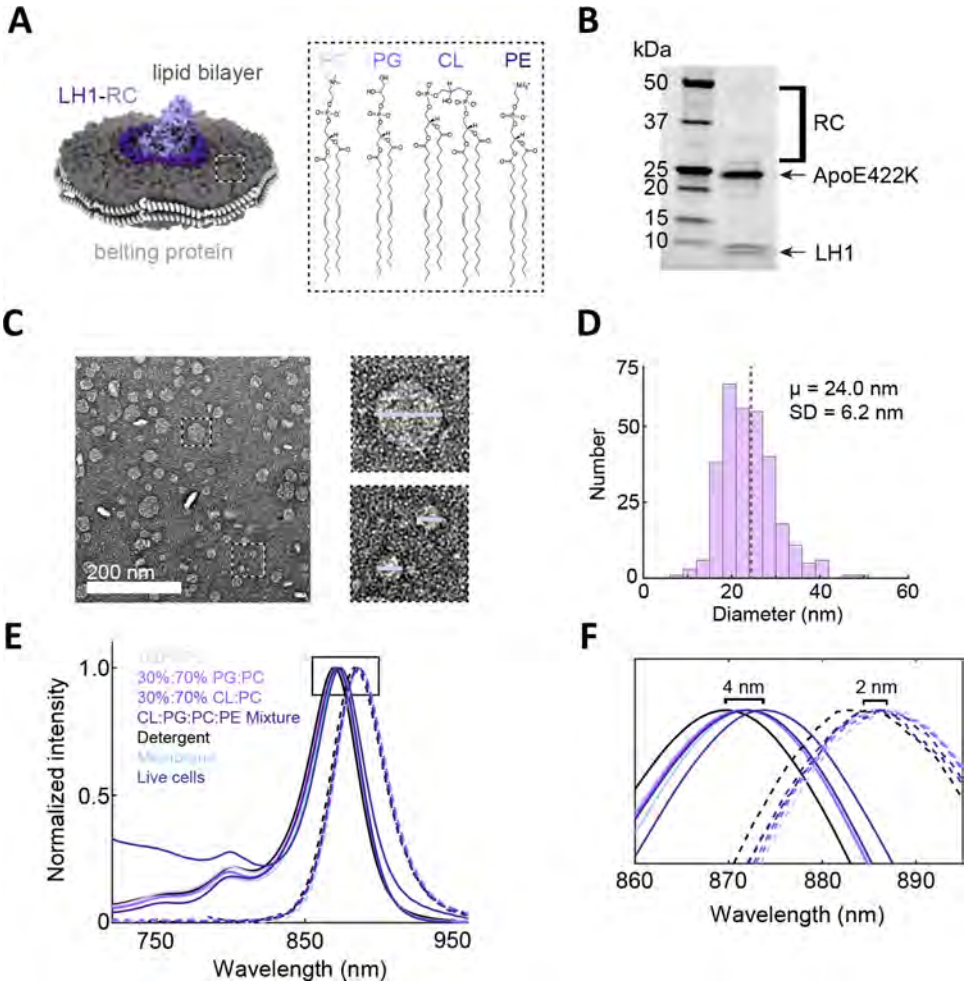

Figure 1. Reconstitution of LH1-RC into nanodiscs. (A) Schematic of LH1-RC (purple, PDB 3WMM) embedded in a nanodisc (left) with the membrane (dark gray) stabilized by an encircling belting protein (light gray) and the lipid structures, right; phosphatidylcholine (PC) (zwitterionic), phosphatidylglycerol (PG) (anionic), cardiolipin (CL) (anionic), and phosphatidylethanolamine (PE) (zwitterionic). (B) Sodium dodecyl-sulfate polyacrylamide gel electrophoresis (SDS-PAGE) of LH1-RC in 100 mol % PC nanodiscs showing the LH1-RC subunits and ApoE422K belting protein. (C) Representative transmission electron microscopy (TEM) micrograph showing individual nanodiscs (dotted line callouts). The scale bar (white) is 200 nm. (D) Corresponding histogram of nanodisc diameters from TEM images (N = 305). The gray dotted line indicates the mean. (E) Absorption (solid lines) and fluorescence emission (dashed-dotted lines) spectra of LH1-RC in detergent (black), 100 mol % PC (neutral) (light pink), 30:70 mol % PG:PC (light purple) (anionic), 30:70 mol % CL:PC (medium purple) (anionic), and 6:36:25:33 mol % CL:PG:PC:PE (dark purple) (anionic) nanodiscs, native membranes (light blue), and live cells (dark blue). The excitation wavelength of the emission spectra is 532 nm. (F) Zoom-in of the B870 absorption and emission peaks, highlighting the 2−4 nm blue shift that occurs in both spectra when LH1-RC is in detergent compared to a membrane.

(BChla) and one carotenoid.[21−25] The BChla-containing proteins form a ring absorbing at ∼870 nm, called the B870 ring.[26−28] The RC contains three protein subunits that bind four BChlas and two bacteriopheophytin (BPhe).[2,29] Two of the BChlas form the so-called special pair (P),[2,30,31] with the rest of the cofactors organized into two branches, A and B, each with one accessory BChla, one BPhe, and one quinone. The quinones are denoted Q_A or Q_B for their associated branch.[2]

In purple bacteria, LH1-to-RC energy transfer is the rate-limiting step in solar energy conversion with a time scale of 30−60 ps.[32−36] Once the photoenergy reaches the RC, the initial charge separation occurs at P, followed by a series of electron-transfer steps down the A branch to Q_A and finally to Q_B. After rereduction of P, another cycle results in the conversion of Q_B to a quinol. The quinol exits LH1-RC to drive the rest of the cyclic electron transport chain. A fresh quinone from the quinone pool replaces Q_B, "turning over" the RC.[29] An RC with P and the quinones in the neutral state is known as "open," whereas an RC with P in the oxidized state (P^+ and either Q_A or Q_B in the reduced state Q^-) is known as "closed," as it cannot perform another electron transfer until P is rereduced by cytochrome.[36−38] In a closed LH1-RC, energy can still transfer from LH1 to an RC with P in the oxidized state, but with a slower overall time scale of 200−300 ps.[36,39−41] While this detailed picture of the molecular composition and the resultant energy and electron-transfer pathways of LH1-RC has been well established, knowledge of the complex and dynamic surrounding lipid bilayer is much more limited. Understanding the functional role of these lipids in solar energy conversion requires new experiments that directly probe their impact.

In this work, we quantified the impact of the lipid composition on LH1-to-RC energy transfer, which is sensitive to RC turnover. By incorporating LH1-RC from *Rsb. denitrificans* into model membrane discs, termed "nanodiscs,"[42]

https://doi.org/10.1021/jacs.5c12301
J. Am. Chem. Soc. 2025, 147, 36706−36716

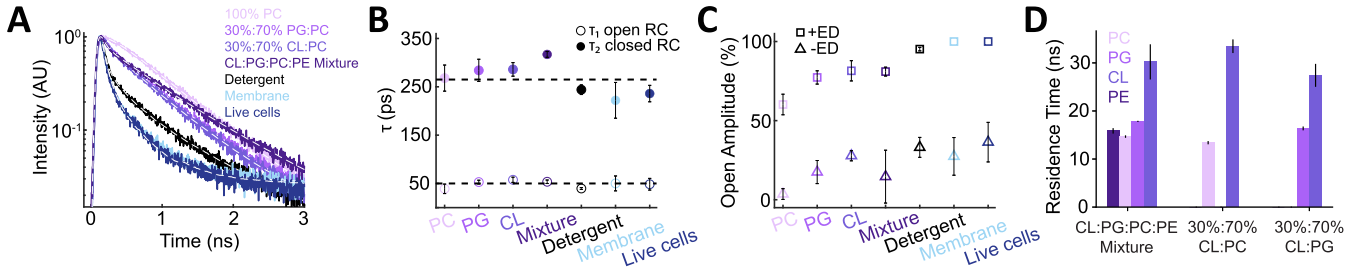

Figure 2. Fluorescence lifetime data of LH1-RC in different environments. (A) Time-correlated single photon counting (TCSPC) traces of LH1-RC in the presence of the electron donor (+ED). The data (solid lines) are overlaid with the fitting results (dotted lines). (B) Time scales of energy transfer in open (τ_1, open circles) and closed (τ_2, closed circles) RCs based on the fluorescence lifetime fitting results. The dotted lines indicate the average for each time scale (τ_1 = 50 ps; τ_2 = 265 ps). (C) Amplitudes of the open RC component (τ_1) in the presence (squares) and absence (triangles) of the electron donor. All error bars are the standard deviations of three independent LH1-RC and nanodisc preparations. (D) Residence time of different lipids around LH1-RC as calculated by coarse-grained MD simulations in the 5−8 Å cutoff range. Tabulated binding durations for other cutoffs are reported in Tables S8−S11. The error bars represent the standard deviations of three replicates, discounting the first 5 μs as an equilibration. The duration of the simulation is 55 μs.

we introduced a tunable lipid environment. Using time-resolved fluorescence and transient absorption (TA) spectroscopy, we quantified the LH1-to-RC energy transfer rates in detergent, in 100 mol % PC (neutral), 30:70 mol % PG:PC (anionic), 30:70 mol % CL:PC (anionic), and 6:36:25:33 mol % CL:PG:PC:PE mixture membrane (anionic) nanodiscs as well as in native membranes and intact cells. While the LH1-to-RC energy transfer rates are independent of lipid composition, the data suggest that RC turnover is significantly hindered in neutral bilayers yet nearly recovers in partially anionic ones. Using molecular dynamics (MD) simulations, we showed that cardiolipin forms long-lasting electrostatic interactions with basic amino acids in the LH1 ring, likely maintaining an open quinone exchange channel for RC turnover. Although anionic phospholipids are a minority component of the bilayer, our experimental and computational results suggest that they are required to maintain robust electron flow, explaining the functional rationale behind the observations of their affinity for LH1-RC.

RESULTS

Nanodisc Formation and Steady-State Characterization of LH1-RC. *Rsb. denitrificans* DSM7001 Δpuc is a knockout mutant for the peripheral antenna complex, light-harvesting complex 2 (LH2),[43] which allows biochemical and spectroscopic studies focusing on LH1-RC and production of purified LH1-RC in sufficient quantity for spectroscopy experiments in nanodiscs. Intact cells, LH1-RC-containing membranes, and isolated LH1-RC were all prepared from this cell line. Isolated LH1-RC was prepared in *n*-dodecyl-β-D-maltoside (DDM), a nonionic detergent. Three nanodisc samples were produced with increasing anionic lipid content: 100 mol % PC (zwitterionic), 30:70 mol % PG:PC (anionic), and 30:70 mol % CL:PC (anionic). These three lipids are the most prominent found in *Rsb. denitrificans*[12] and similar to the relative abundances of the lipid charge ratios typically observed in purple bacteria.[7,13] We chose an approximate 30:70% anionic:neutral mixture in the nanodiscs to replicate the percentages typically seen in the photosynthetic membranes of purple bacteria.[6] Finally, to more precisely replicate the broad lipid distribution found in many species of purple bacteria, we also prepared a fourth nanodisc sample with a 6:36:25:33 mol % CL:PG:PC:PE lipid composition.[6] Successful nanodisc formation was confirmed by transmission electron microscopy (TEM), SDS-PAGE, and steady-state spectroscopy (Figure 1B−F). Analysis of the TEM micrographs (Figure 1C) was used to find the distribution of nanodisc diameters (Figure 1D), which were ∼20 nm for all lipid compositions (Figure S2). The nanodisc size allowed for one LH1-RC (11.8 nm diameter) to be incorporated per disc.[44] The steady-state spectra for LH1-RC in detergent, nanodiscs, native membranes, and live cells are overlaid in Figure 1E. Similar features were observed in all samples, confirming that the integrity of the LH1-RC was generally retained upon nanodisc formation. The large peak at 870 nm is from the LH1 BChla[27,28] and exhibits a slight blue shift (∼2−4 nm) in detergent, similar to previous studies on purple bacterial proteins (Figure 1F).[10,45−47]

Time-Resolved Spectroscopy Reveals that RC Turnover Depends on Lipid Environment. The time scale of LH1-to-RC energy transfer can be observed through the decay of LH1 fluorescence. This energy transfer step is orders of magnitude slower than the subsequent charge separation or quenching by oxidized P in the RC,[36] and so it dominates the fluorescence decay time scale. Under typical laser conditions for time-resolved experiments, the photon fluence and repetition rate excite LH1-RC at a rate higher than the RC recovery time,[36] leading to closed RCs. The addition of an electron donor (ED) to the buffer, such as ascorbate and phenazine methosulfate, rereduces P and oxidizes the quinones,[32,38,40,48,49] leading to open RCs. Fluorescence lifetime measurements were performed both with and without the electron donor for LH1-RC under six conditions: detergent; nanodiscs with the four lipid compositions; native membranes; and live cells. Excitation was tuned to the red tail of the LH1 absorption band (Figure 1E) to minimize direct excitation of P.[32]

The fluorescence lifetime traces for all conditions are shown in Figures 2A and S5, with the corresponding fit values provided in Tables S1 and S2. For the purified LH1-RC samples (detergent and nanodiscs), the decays were globally fit by a triexponential function with the values of the first (τ_1) and second (τ_2) time constants shared between buffer conditions. τ_1, ∼40−60 ps, corresponded to energy transfer to open RCs,[32−36] while τ_2, ∼240−320 ps, corresponded to energy transfer to closed RCs.[36,39−41] The third time constant, τ_3, was allowed to vary across the sample conditions. τ_3, ∼600−1200 ps, corresponded to free LH1 emission with values in agreement with previous reports.[36,50−52] The broad range of free LH1 lifetimes is likely due to the greater flexibility in the

https://doi.org/10.1021/jacs.5c12301
J. Am. Chem. Soc. 2025, 147, 36706−36716

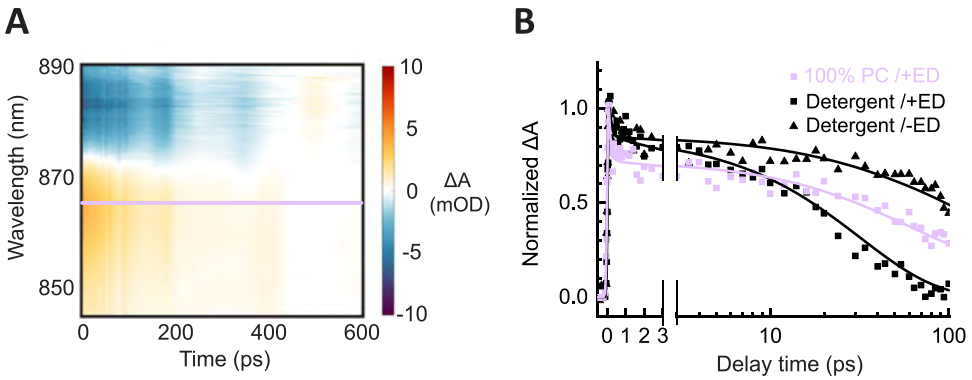

Figure 3. Transient absorption data of LH1-RC in different environments. (A) Two-dimensional (2D) representation of TA data in 100 mol % neutral PC nanodiscs in the presence of the electron donor system (+ED). Color bar (ΔA, mOD) represents signal intensity. (B) Single-wavelength transients of the TA data at 865 nm (pink line in (A)) for the three sample conditions: 100 mol % PC nanodiscs in the presence of the electron donor (+ED) (pink squares), detergent in the presence of the electron donor (+ED) (black squares), and detergent in the absence of the electron donor (−ED) (black triangles). The fits are displayed as solid lines.

absence of the RC, which allows local charge and other interactions to influence its conformation.[53,54] The electron donor also introduces a small scattering signal that can influence the third time component. For the anionic nanodiscs and detergent conditions, the amplitude of the free LH1 emission is small (<13%) (Table S1), indicating the majority of LH1-RC complexes are intact. The amplitude increased to ∼30% for the 100 mol % PC nanodiscs, suggesting that LH1-RC is less stable and/or harder to incorporate into the neutral bilayer. This is in agreement with previous studies on LH1-RC.[14,47]

For the membrane and live cell samples, the decays were globally fit by a biexponential function, with the values of the first time constant (τ_1) shared between buffer conditions. τ_1, ∼50 ps, again corresponded to energy transfer to the open RCs. In the presence of the electron donor, there was a nearly 100% amplitude of this fast time constant (Table S1). A small component due to scattering from the presence of the electron donor was assigned as the second component. In the absence of the electron donor, τ_2, ∼220−240 ps, again corresponded to energy transfer to closed RCs (Table S2). The similar LH1-to-RC energy transfer time scales for all samples (Figure 2B) indicated that the membrane environment does not have a significant effect on this process. Specifically, the similarity of these time scales suggests that similar, intact LH1-RC complexes are maintained under all lipid conditions with changes in the relative populations of the open and closed forms.

From the amplitudes of the two fast components (i.e., LH1-to-RC energy transfer), the percents of LH1-RC in the open state were calculated (Figure 2C). For all samples, the open state dominates in the presence of the electron donor, whereas the closed state dominates without the electron donor (Tables S1 and S2), consistent with the role of the electron donor in enabling redox cycling. For the detergent, native membranes, and live cells, the samples were almost entirely (>90%) in the open state with the electron donor (Figure 2C), indicating full redox cycling, and partially (∼30%) in the open state without the electron donor. For the reconstituted membrane environments, the amplitudes showed samples only partially in the open state, both with and without the electron donor. For the neutral PC nanodiscs with the electron donor, the samples are 60% in the open state. For the anionic PG and CL nanodiscs with the electron donor, samples are 77 and 82%, respectively, suggesting anionic lipid content is important in mimicking the properties of the native membranes. In line with the two-component anionic nanodisc samples, the CL:PG:PC:PE lipid mixture nanodisc samples are 81% in the open state. The mixture of open and closed states without the electron donor was expected, as the laser shifts the population into the closed state in a power and repetition rate-dependent manner.[36] In contrast, the mixture of states with the electron donor was unexpected, as it suggests that full redox cycling cannot be achieved with these lipids.

To more directly investigate the excited-state dynamics, we also used TA spectroscopy to probe LH1-RC in detergent and in 100 mol % PC nanodiscs, which has a higher time resolution (0.1 ps) than fluorescence lifetime measurements (88 ps) and, therefore, enables higher precision measurements. These two samples were selected to span the behaviors observed in the fluorescence lifetime measurements: LH1-RC in detergent exhibited the nearly native open state percentage yet lacked the scattering background of measurements on native membranes or live cells; and LH1-RC in 100 mol % neutral PC nanodiscs exhibited the largest closed state percentage with the electron donor. Similar to the fluorescence lifetime measurements, excitation was tuned to the red tail of the LH1 absorption band (880 nm, Figure S8). Representative TA data for LH1-RC in 100 mol % PC nanodiscs with the electron donor are shown in Figure 3A. The data without the electron donor and in detergent are shown in Figure S9.

The TA data were fit globally with a sum-of-exponential decay model. Representative transients at 865 nm for the three conditions are compared in Figure 3B, with the full data analysis shown in Figure S9. In the presence of the electron donor, the 100 mol% neutral PC nanodiscs displayed four components: 0.12 ps, corresponding to equilibration of LH1;[32] 44 ps, corresponding to LH1-to-RC energy transfer in the open state, 280 ps, corresponding to LH1-to-RC energy transfer in the closed state, and 720 ps, corresponding to LH1 emission.[36] In detergent, the data was reduced to only the two short components: 0.12 ps (LH1 equilibration) and 32 ps (LH1-to-RC energy transfer in the open state). In the absence of the electron donor, the detergent sample displayed three components: the fast 0.12 and 32 ps components as well as a slow 260 ps component.

While the 0.12 ps component cannot be resolved in our fluorescence lifetime experiments, the other three components

https://doi.org/10.1021/jacs.5c12301
J. Am. Chem. Soc. 2025, 147, 36706−36716

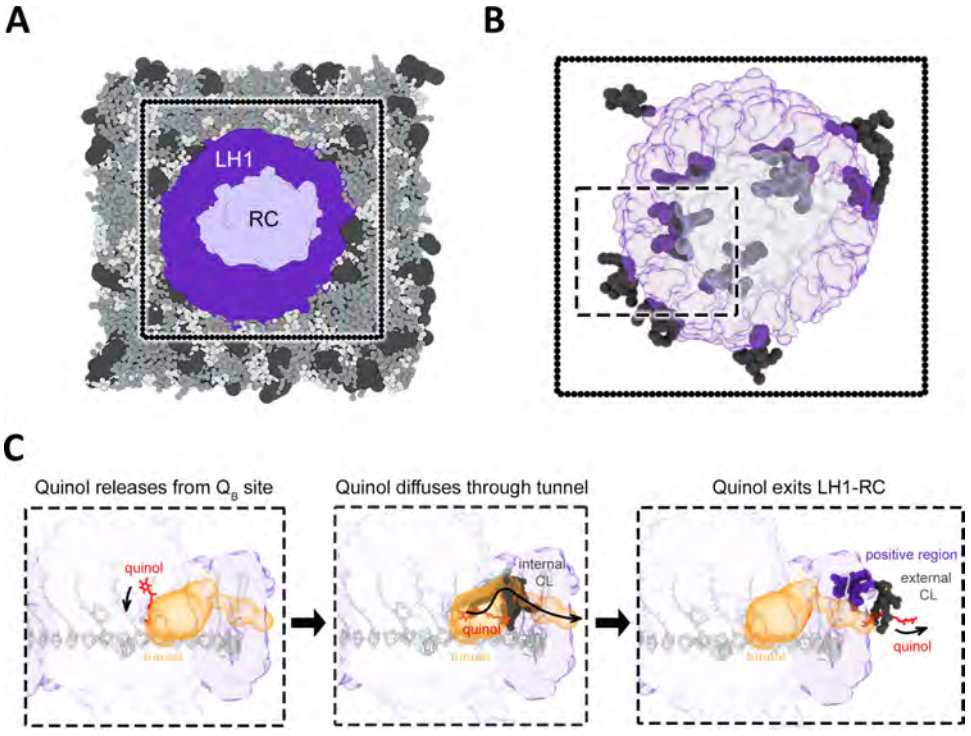

Figure 4. Cardiolipins play a facilitating role in LH1-RC quinone diffusion. (A) Molecular dynamic simulation results of lipid interactions with LH1-RC. Cardiolipins (CL) are emphasized using large, dark gray ball representation. (B) Zoom-in on LH1-RC, showing external CLs interacting with the LH1-RC from the MD simulation and the respective CLs which are internally bound to LH1-RC (based on PDB code 5Y5S structure). (C) Snapshots of suggested quinol (red stick representation) diffusion pathway from the Q_B site out of the LH1 ring, mediated by the internal- and external-interacting CLs (dark gray). The region of LH1-RC depicted is outlined by the dotted lines also shown in panel (B). The tunnel (orange volume), as calculated by the MOLE server, is a region without a protein backbone that partially overlaps with the lipid tails and connects the Q_B binding site with the membrane environment. The specific residues facilitating external CL binding (purple) are highlighted. The left panel shows the quinol releasing from the Q_B binding site; the middle panel shows the quinol diffusing through the tunnel, and the right panel shows the quinol moving out of the tunnel through the LH1 ring.

measured by TA agree well with those found by the fluorescence lifetime measurements. In particular, the LH1-to-RC energy transfer components for both open and closed RCs even in the presence of the electron donor again indicated that redox cycling was unexpectedly impeded in the 100 mol% neutral PC nanodiscs. The TA measurements confirmed the behaviors observed in our fluorescence lifetime measurements.

MD Simulations Identify LH1-CL Interactions. The disrupted RC turnover in nanodiscs compared to native membranes strongly suggested preferential lipid interactions with the LH1 ring. To investigate the specificity of these lipid interactions, we performed three sets of coarse-grained MD simulations of LH1-RC: (1) CL, PG, PC, PE lipids in a 6:36:25:33% ratio (shown in Figure 4A), (2) CL, PC in a 30:70% ratio, and (3) CL, PG in a 30:70% ratio. The first two mixtures replicated our nanodisc samples, while the third probed the specific influence of CL versus PG. Simulations were also performed without ubiquinone as a control (Figure S17). As the structure of LH1-RC from *Rsb. denitrificans* has not yet been resolved, we made a homology model (Figure S10) based on the structure of *Thermochromatium (Tch.) tepdium*,[18] which is a 16-mer LH1 $\alpha\beta$ ring with H, L, M, and cytochrome RC subunits. LH1-RC from *Tch. tepidum* has the highest resolution of available structures and lacks the pufX gene, resulting in a closed ring consistent with current models of LH1-RC from *Rsb. denitrificans*. Homology modeling is widely used to interpret results on proteins for which no structure is yet available.[55−61] Table S3 shows relatively high sequence identity between the LH1-RC subunits of *Tch. tepidum* and *Rsb. denitrificans*, which is typically suggestive of homologous structures.[62,63] It has been found that when modeling membrane proteins, using a template structure with at least 30% sequence identity will generally yield an acceptable C-alpha root mean squared deviation (RMSD) value of less than 2 Å between the predicted structure and the true structure in the transmembrane regions.[64]

The MD trajectories showed the LH1-RC surrounded by a lipid bilayer with a dynamic local lipid composition. From the simulations, the duration of each lipid surrounding the exterior of the LH1-RC, termed "residence time," was determined by quantifying how long until the lipid exceeds a threshold from the LH1 ring (8 Å) after coming within 5 Å (Figures 2D, S17, and S18, Tables S8−S11). In all of the simulations, the average residence time for anionic PG was slightly longer than that for the neutral PC and neutral PE, and the time for anionic CL was almost twice as long, indicating that the times were longer for anionic phospholipids. The significantly longer residence time for CL compared to other lipids is consistent with the strong affinity for anionic CL to LH1-RC previously reported in the literature.[6,17]

To further investigate the specificity of the lipid−protein interactions, the distributions of residence times were plotted for each lipid (Figures S19−S22). A single-component decay profile was observed for neutral PC, indicating no specific interactions between PC and the LH1 ring. In contrast, an additional slower decay component was present for anionic

https://doi.org/10.1021/jacs.5c12301
J. Am. Chem. Soc. 2025, 147, 36706−36716

CL, reflecting a subpopulation that remained bound on the outside of the LH1 ring for over a microsecond. A similar subpopulation was present for PG, but with a much lower amplitude. Analysis of the simulation results revealed that this subpopulation of long-lived bound CL is due to a cluster of eight residues on the external LH1 ring. These residues have a net positive charge (F4, K3, K6, M68, S69, H64, W8, and Q61). The interactions between this cluster and CL are shown in Figure 4B.

DISCUSSION

LH1-RC Dynamics Change with Lipid Environment. The LH1-to-RC energy transfer time scales were ∼50 and ∼260 ps for open and closed RCs, respectively, in agreement with previous studies.[32−36,39−41] Our results are the first direct comparison between detergent and different membranes. The same values were observed under all conditions, establishing that the time scale of this key step is not influenced by the local molecular environment. This consistency is particularly notable, as other photosynthetic proteins, such as LHCII in green plants[11] and LH2 in purple bacteria,[10] show membrane-dependent energy transfer time scales. These proteins also exhibited shorter fluorescence lifetimes in membranes, whereas the free LH1 component was consistent between the detergent and membrane samples in the absence of the electron donor (Table S2). In the presence of the electron donor, membrane samples had shorter lifetimes, similar to other photosynthetic proteins, but the small amplitude (<5%) of the free LH1 component in detergent makes it challenging to draw definitive conclusions. In accordance with the consistent time scales of the LH1-RC, the MD simulations of the protein show that the pigments are embedded within the protein without any distortion as nearby lipids exchange. The LH1-to-RC energy transfer step is the rate-limiting step of solar energy conversion in purple bacteria. RC-to-LH1 back transfer is much faster to allow the excitation to reach other RCs if the first one is closed.[37,38,65−69] The conservation of this rate-limiting time scale across a variety of membrane conditions, as demonstrated in our experiments, may reflect that this step is key for overall high quantum efficiency in photosynthetic light harvesting.

In contrast to the LH1-to-RC energy transfer rate, the turnover of the RC depends strongly on the lipid environment. Even in the presence of electron donors, such as ascorbate and phenazine methosulfate, which are expected to maintain an open LH1-RC, the population of LH1-RC complexes in the open state can drop dramatically. This indicates that normal RC redox cycling was disrupted. The disruption was the most dramatic for the neutral PC bilayer. Adding the anionic lipids PG and CL increased the population of LH1-RC complexes in the open state, indicating that redox cycling was partially restored. In detergent, the population of LH1-RC complexes in the open state was very close to native levels, likely because the native, local anionic lipids that maintain the LH1-RC structure and function were retained even in detergent solubilization. This is supported by previous studies that indicate a large proportion of anionic lipids copurify with LH1-RC in detergent[6,17] and cryo-EM structures of LH1-RC that resolve these lipids in similar positions.[19,20,22] When incorporated into nanodiscs, these lipids could be disrupted or displaced by the reconstitution procedure. The LH1-RC sample was solubilized in *n*-dodecyl-*β*-D-maltoside (DDM), a gentle nonionic detergent commonly used to purify membrane proteins, whereas nanodisc reconstitution involved the introduction of lipids solubilized using the anionic detergent cholate. The introduction of the anionic cholate could have disrupted the positioning of the lipids interacting with LH1-RC. Indeed, it has been found that in reconstitution mixtures containing both cholate and DDM, reconstitution is influenced more strongly by the cholate.[70] While a similar dependence may be present for nanodisc formation, additional data would be required to make a definitive assignment. In contrast to the more native-like kinetics, the peak maxima in detergent were blue-shifted as compared to the nanodisc samples and native membranes, which showed similar maxima (Figure 1E). The loss of lateral membrane pressure in detergent may allow for structural relaxation,[10,47] decreasing the pigment−protein interactions that red-shift the pigment transitions in the protein binding pocket.[71] Together, these results suggest that the membrane environment introduces both local interactions and mechanical forces. Thus, a proper choice of solubilization environment is critical in the study of native protein structure and function and may need to be carefully selected based on the parameter under investigation.

The unexpected disruption of redox cycling by neutral lipids likely occurred at one of the two charged cofactors, P and the quinone, in the charge-separated state. P is rereduced through a series of electron-transfer steps initiated by soluble electron donors, which interact in solution with the RC cytochrome *C* subunit that protrudes out of the membrane and so are unlikely to have membrane dependence.[2,72] In contrast, the quinone, now reduced to its quinol form, exits the LH1-RC within the lipid bilayer, making it the likely site of lipid-dependent disruption.

Quinone Exchange through LH1-RC May Be Facilitated by Cardiolipin. Across species of purple bacteria, there are two main classes of LH1-RC structures, distinguished by the structure of their LH1 rings: open, where some LH1 subunits are "missing," creating a gap in the ring to facilitate quinone entry and exit; and closed, where the LH1 completely surrounds the RC. The open structures often contain proteins in the gap that are thought to create a pathway to direct quinone diffusion.[20,24,73−79] How quinone diffusion occurs through closed LH1 ring structures has been puzzling.

Both open and closed LH1-RC structures have shown that lipids preferentially orient in specific positions in the space between the LH1 ring and the RC. The resolution of lipids in the LH1-RC structures indicates that they are sufficiently bound to remain associated even with DDM solubilization. Lipid and detergent molecules resolved by structural biology are also likely to be less dynamic and to be more vital to the complex. Anionic CLs have been observed on the cytoplasmic side with their headgroups positioned toward the membrane surface closer to the quinone binding site, whereas detergent and neutral lipids generally were seen to associate on the periplasmic side, farther away from the quinone binding site.[18−20,22] In particular, CLs are consistently resolved[6,20] and have been the most common lipids found with LH1-RC upon purification,[6] consistent with the longer residence times of CL in the MD simulations (Figures 2D, S17, and S18).

Although the atomic structure of LH1-RC from *Rsb. denitrificans* has not yet been resolved, atomic force microscopy (AFM) images indicated that it has a closed structure.[44] Furthermore, *Rsb. denitrificans* lacks the pufX gene that encodes PufX,[80] the protein most often responsible for creating the open LH1 ring.[2] PufX is believed to have evolved from an extended version of the N-terminal domain of the RC

https://doi.org/10.1021/jacs.5c12301
J. Am. Chem. Soc. 2025, 147, 36706−36716

cytochrome subunit, which is still present in species such as *Rsb. denitrificans* and *Rhodopila (Rpi.) globiformis*. The structure of *Rpi. globiformis* was recently resolved and found to be a closed structure.[81] Closed structures from other species have shown that the regions between the LH1 α and β subunits form small hydrophobic channels that could allow for the passage of quinone molecules into and out of LH1-RC.[18,19,22,81]

For *Tch. tepidum*, it was found that these regions contain CL molecules that interact with basic residues on the LH1 α polypeptides, for example, two arginine residues (R18 and R19).[6,18] The strong association of the anionic CL headgroups with basic residues is what is believed to strengthen the interaction between the LH1 and RC and facilitate quinone diffusion through these channels.[6,18,82] In fact, the pair of arginine residues is conserved across the sequences of at least 12 species (Figure S23). Our homology model of *Rsb. denitrificans* shows a similar positioning of these residues that interact internally with cardiolipin at the channel sites (Figure S10D). Recent work monitoring quinone exchange in *Tch. tepidum* also showed interaction with the surrounding protein in a membrane-dependent manner, consistent with a role of both protein channels and lipids in quinol exit.[82] Our MD simulation, which contains ubiquinones in the space between LH1 and the RC, has shown the exit of the ubiquinol molecule from the reaction center to the lipid membrane through the LH1 ring, as shown in Movie 1. Observation of this exit requires significant computational time; consequently, we lack sufficient sampling behind the exit. Therefore, it can currently only be categorized as a rare event. However, observation of this exit shows that it is possible for ubiquinol to exit the LH1 ring, and future simulations will explore this observation in more detail.

The high affinity of anionic lipids to LH1-RC could explain why the detergent-solubilized LH1-RC has the turnover rate closest to the native membranes, as the associated native lipids are likely maintained (Figure 2C). Lipids are thought to play a role in maintaining LH1-RC integrity, and a higher proportion of LH1-only complexes were observed in the nanodiscs (Tables S1 and S2), consistent with a loss of interacting lipids during reconstitution. In the PC nanodisc, the proportion of disrupted complexes was the highest, potentially because the zwitterionic headgroup results in more complicated and heterogeneous lipid−protein interactions as well as a less hydrophobic environment that would slow down quinone diffusion. Addition of the anionic PG and CL increased LH1-RC turnover, potentially due to restoration of the native hydrophobic environment with associated anionic lipids.

Our findings strongly suggest that anionic lipids play a role in the redox properties of LH1-RC, likely through facilitating the quinone cycle. Anionic lipids, particularly CL, preferentially bind externally to the LH1 ring in the MD simulations through interaction with the basic residues, whereas previously reported structures indicated that CL binds internally to the LH1 ring.[18,20] These sites are at opposite positions across the hydrophobic channel (Figure 4C). We hypothesize that quinone diffusion through the channel may be facilitated by the anionic CLs at the entry and exit sites, such as through an exchange process. Future experiments, such as with cationic lipids, could further investigate whether these specific interactions play a role. Even in open LH1-RC ring structures, the quinone can move through both the gaps and through the opening,[83] though transport is accelerated through the ring opening as diffusion is faster and more energetically favorable through the bulk membrane than the hydrophobic channels.[20,83] The presence of anionic lipids, which may also associate at the ring opening, could again help facilitate quinone transport out of the complex.

It is additionally possible that anionic lipids like CL and PG affect the kinetics of quinone binding and unbinding at the RC. Previous studies have found that CL and PG stabilize the $P^+Q_B^-$ charge-separated state,[14,17] and a cryo-EM study that compared LH1-RC from three species of purple bacteria found a conserved region of CL near the Q_A binding site.[20] While more work is needed to resolve the specific interactions at the quinone binding sites, it is very possible that anionic lipids like CL facilitate the entire quinone transport and binding/unbinding process within LH1-RC: they could direct quinone diffusion through the LH1 ring toward the quinone binding site and/or stabilize charge separation at the RC, possibly due to modification of the Q_A or Q_B redox potential by the anionic lipids.[15−17,84] Consistent with this picture, the charge-separated state was destabilized at high pH. This was attributed to changes in electrostatic interactions between the charged and aromatic residues, CL, and the quinone pool between LH1 and the RC.[17] The interactions between these three charged species (quinones, lipids, and protein) likely work together to maintain cyclic electron transport through the LH1-RC complex. Future work can combine simulation and experiment for a single species of purple bacteria to explore these mechanisms in more detail, with further comparisons across multiple species with different ring structures.

CONCLUSIONS

In summary, we combined time-resolved spectroscopy, biochemistry, and MD simulations to determine the impact of lipids on the LH1-RC function by tuning the surrounding lipid composition with the nanodisc platform. While the LH1-to-RC energy transfer rate is consistent regardless of the surrounding lipids, RC turnover appears to require anionic lipids, suggesting that lipid composition mediates electron carrier exit from the LH1-RC. These results illustrate that the membrane environment must not be ignored: lipids are not solely a matrix in which proteins sit but can play an active role in biological processes, and in photosynthesis, membrane conditions are optimized to facilitate an efficient electron turnover, potentially in a manner involving pH, redox potential, and/or membrane potential. LH1-RC is particularly fascinating because its structure can vary widely across species; however, key components are preserved, including the LH1-to-RC energy transfer rate and the lipid immediately surrounding the complex.

It would be interesting to compare these lipid effects with species containing open LH1-RC structures, such as that from *Rhodopseudomonas (Rps.) palustris*, which can form both open and closed LH1 rings,[20] or *Rhodobacter sphaeroides*, which has open rings and can form dimeric or monomeric structures.[79] It has been found that *Rps. palustris* can form different ratios of open and closed structures depending on light conditions,[20] potentially to fine-tune quinone transport in response to fluctuating light conditions. Purple bacteria may combine these two parameters, ring structure and membrane composition, to balance quinone transport and thus maintain stable solar energy conversion.

https://doi.org/10.1021/jacs.5c12301
J. Am. Chem. Soc. 2025, 147, 36706−36716

■ ASSOCIATED CONTENT

Supporting Information

The Supporting Information is available free of charge at https://pubs.acs.org/doi/10.1021/jacs.5c12301.

Experimental details, fast protein liquid chromatograms (FPLC) of nanodisc purification, nanodisc size distributions from transmission electron microscopy, full linear absorption spectra, stability comparison of 100 mol % PC and 30:70 mol % CL:PC nanodisc samples, fluorescence lifetime fitting parameters, fluorescence lifetime data and fits in the absence of the electron donor system, fits and residuals of fluorescence lifetime data, transient absorption pulse generation, transient absorption data and analysis, homology model of LH1-RC, sequence identity comparison of *Tch. tepidum* and *Rsb. denitrificans*, coarse-grained simulation details, time-dependent evolution of lipid types in the MD simulation, depletion−enrichment index data, residence time data for all simulations, survival probability plots for all simulations, and a comparison of LH1 α sequences (PDF)

Ubiquinol exit from LH1 ring (MP4)

■ AUTHOR INFORMATION

Corresponding Author

Gabriela S. Schlau-Cohen − *Department of Chemistry, Massachusetts Institute of Technology, Cambridge, Massachusetts 02139, United States;* orcid.org/0000-0001-7746-2981; Email: gssc@mit.edu

Authors

Olivia C. Fiebig − *Department of Chemistry, Massachusetts Institute of Technology, Cambridge, Massachusetts 02139, United States;* Present Address: Department of Chemistry, Smith College, Northampton, Massachusetts 01063, United States; orcid.org/0000-0002-5265-1636

Graham P. Schmidt − *Department of Chemistry, Massachusetts Institute of Technology, Cambridge, Massachusetts 02139, United States*

Neetu Singh Yadav − *MSU-DOE Plant Research Laboratory, Michigan State University, East Lansing, Michigan 48824, United States;* orcid.org/0000-0002-4535-4959

Dihao Wang − *Department of Chemistry, Massachusetts Institute of Technology, Cambridge, Massachusetts 02139, United States;* orcid.org/0000-0002-3866-0077

[⊥]Muath Nairat − *Department of Chemistry, Massachusetts Institute of Technology, Cambridge, Massachusetts 02139, United States*

Helen Tang − *MSU-DOE Plant Research Laboratory, Michigan State University, East Lansing, Michigan 48824, United States*

Yi Ji − *Department of Chemistry, Massachusetts Institute of Technology, Cambridge, Massachusetts 02139, United States*

Valérie Prima − *LISM UMR 7255, CNRS and Aix-Marseille University, Marseille 13402, France*

James N. Sturgis − *LISM UMR 7255, CNRS and Aix-Marseille University, Marseille 13402, France;* orcid.org/0000-0001-5125-7699

Josh V. Vermaas − *MSU-DOE Plant Research Laboratory, Michigan State University, East Lansing, Michigan 48824, United States;* orcid.org/0000-0003-3139-6469

Dvir Harris − *Department of Chemistry, Massachusetts Institute of Technology, Cambridge, Massachusetts 02139, United States*

Complete contact information is available at: https://pubs.acs.org/10.1021/jacs.5c12301

Notes

The authors declare no competing financial interest.

[⊥]Deceased Feb 9, 2024.

■ ACKNOWLEDGMENTS

This work was primarily supported by the U.S. Department of Energy, Office of Science, Office of Basic Energy Sciences, Division of Chemical Sciences, Geosciences, and Biosciences under Award DE-SC0018097 to G.S.S.-C. J.V.V. was supported in part by the U.S. Department of Energy, Office of Basic Energy Sciences under grant number DE-FG02-91ER20021. The project leading to this publication has also received funding from the Excellence Initiative of Aix-Marseille University—A*Midex, a French "Investissements d'Avenir" programme. O.C.F. acknowledges support from an NSF Graduate Research Fellowship. D.H. acknowledges the Yad Hanadiv (Rothschild) Foundation, the Zuckerman STEM Leadership Program, and the Israel Council for Higher Education (CHE) for their generous financial support. G.S.S.-C also acknowledges support from a Camille Dreyfus Teacher-Scholar Award. The authors thank Prof. Moungi Bawendi for help with the near-infrared fluorescence measurements. This work made use of the MRSEC Shared Experimental Facilities at MIT, supported by the National Science Foundation under award number DMR-1419807. This work was supported in part through computational resources and services provided by the Institute for Cyber-Enabled Research at Michigan State University. A previous version of this work originally appeared in the Ph.D. thesis of O.C.F.[85] This paper is dedicated to the memory of Dr. M.N., who built the spectrally resolved transient absorption setup used in this work and performed some initial transient absorption experiments on LH1-RC. He was an outstanding scientist, kind and supportive colleague, and a good friend. He will be greatly missed.

■ REFERENCES

(1) Hu, X.; Damjanović, A.; Ritz, T.; Schulten, K. Architecture and mechanism of the light-harvesting apparatus of purple bacteria. *Proc. Natl. Acad. Sci. U.S.A.* **1998**, *95*, 5935−5941.

(2) Liu, L.-N.; Bracun, L.; Li, M. Structural diversity and modularity of photosynthetic RC-LH1 complexes. *Trends Microbiol.* **2024**, *32*, 38−52.

(3) van Grondelle, R.; Dekker, J. P.; Gillbro, T.; Sundström, V. Energy transfer and trapping in photosynthesis. *Biochim. Biophys. Acta, Bioenerg.* **1994**, *1187*, 1−65.

(4) Tamot, B.; Benning, C. *The Purple Phototrophic Bacteria*; Hunter, C. N.; Daldal, F.; Thurnauer, M. C.; Beatty, J. T., Eds.; Springer: Netherlands: Dordrecht, 2009; pp 119−134.

(5) Imhoff, J. F.; Bias-Imhoff, U. *Anoxygenic Photosynthetic Bacteria*; Blankenship, R. E.; Madigan, M. T.; Bauer, C. E., Eds.; Springer: Netherlands: Dordrecht, 1995; pp 179−205.

(6) Nagatsuma, S.; Gotou, K.; Yamashita, T.; Yu, L.-J.; Shen, J.-R.; Madigan, M.; Kimura, Y.; Wang-Otomo, Z.-Y. Phospholipid distributions in purple phototrophic bacteria and LH1-RC core complexes. *Biochim. Biophys. Acta, Bioenerg.* **2019**, *1860*, 461−468.

(7) Benning, C. *Lipids in Photosynthesis: Structure, Function and Genetics*; Paul-André, S.; Norio, M., Eds.; Kluwer Academic Publishers: Dordrecht, 1998; pp 83−101.
(8) Sumino, A.; Dewa, T.; Noji, T.; Nakano, Y.; Watanabe, N.; Hildner, R.; Bösch, N.; Köhler, J.; Nango, M. Influence of phospholipid composition on self-assembly and energy-transfer efficiency in networks of light-harvesting 2 complexes. *J. Phys. Chem. B* **2013**, *117*, 10395−10404.
(9) Dewa, T.; Sumino, A.; Watanabe, N.; Noji, T.; Nango, M. Energy transfer and clustering of photosynthetic light-harvesting complexes in reconstituted lipid membranes. *Chem. Phys.* **2013**, *419*, 200−204.
(10) Ogren, J. I.; Tong, A. L.; Gordon, S. C.; Chenu, A.; Lu, Y.; Blankenship, R. E.; Cao, J.; Schlau-Cohen, G. S. Impact of the lipid bilayer on energy transfer kinetics in the photosynthetic protein LH2. *Chem. Sci.* **2018**, *9*, 3095−3104.
(11) Son, M.; Pinnola, A.; Gordon, S. C.; Bassi, R.; Schlau-Cohen, G. S. Observation of dissipative chlorophyll-to-carotenoid energy transfer in light-harvesting complex II in membrane nanodiscs. *Nat. Commun.* **2020**, *11*, No. 1295.
(12) Hahnke, S.; Tindall, B. J.; Schumann, P.; Simon, M.; Brinkhoff, T. Pelagimonas varians gen. nov., sp. nov., isolated from the southern North Sea. *Int. J. Syst. Evol. Microbiol.* **2013**, *63*, 835−843.
(13) Van Mooy, B. A. S.; Rocap, G.; Fredricks, H. F.; Evans, C. T.; Devol, A. H. Sulfolipids dramatically decrease phosphorus demand by picocyanobacteria in oligotrophic marine environments. *Proc. Natl. Acad. Sci. U.S.A.* **2006**, *103*, 8607−8612.
(14) Noji, T.; Matsuo, M.; Takeda, N.; Sumino, A.; Kondo, M.; Nango, M.; Itoh, S.; Dewa, T. Lipid-controlled stabilization of charge-separated states ($P^+Q_B^-$) and photocurrent generation activity of a light-harvesting-reaction center core complex (LH1-RC) from *Rhodopseudomonas palustris*. *J. Phys. Chem. B* **2018**, *122*, 1066−1080.
(15) Nagy, L.; Fodor, E.; Tandori, J.; Rinyu, L.; Farkas, T. Lipids affect the charge stabilization in wild-type and mutant reaction centers of *Rhodobacter sphaeroides* R-26. *Aust. J. Plant Physiol.* **1999**, *26*, 465−473.
(16) Nagy, L.; Milano, F.; Dorogi, M.; Agostiano, A.; Laczkó, G.; Szebeényi, K.; Váró, G.; Trotta, M.; Maróti, P. Protein/lipid interaction in the bacterial photosynthetic reaction center: Phosphatidylcholine and phosphatidylglycerol modify the free energy levels of the quinones. *Biochemistry* **2004**, *43*, 12913−12923.
(17) Dezi, M.; Francia, F.; Mallardi, A.; Colafemmina, G.; Palazzo, G.; Venturoli, G. Stabilization of charge separation and cardiolipin confinement in antenna-reaction center complexes purified from *Rhodobacter sphaeroides*. *Biochim. Biophys. Acta, Bioenerg.* **2007**, *1767*, 1041−1056.
(18) Yu, L.-J.; Suga, M.; Wang-Otomo, Z.-Y.; Shen, J.-R. Structure of photosynthetic LH1-RC supercomplex at 1.9 Å resolution. *Nature* **2018**, *556*, 209−213.
(19) Tani, K.; Kanno, R.; Makino, Y.; Hall, M.; Takenouchi, M.; Imanishi, M.; Yu, L.-J.; Overmann, J.; Madigan, M. T.; Kimura, Y.; Mizoguchi, A.; Humbel, B. M.; Wang-Otomo, Z.-Y. Cryo-EM structure of a Ca^{2+}-bound photosynthetic LH1-RC complex containing multiple $\alpha\beta$-polypeptides. *Nat. Commun.* **2020**, *11*, No. 4955.
(20) Swainsbury, D. J. K.; Qian, P.; Jackson, P. J.; et al. Structures of *Rhodopseudomonas palustris* RC-LH1 complexes with open or closed quinone channels. *Sci. Adv.* **2021**, *7*, No. eabe2631.
(21) Yu, L.-J.; Ma, F. *Microbial Photosynthesis*; Wang, Q., Ed.; Springer: Singapore, 2020; pp 53−72.
(22) Tani, K.; Kanno, R.; Ji, X.-C.; Hall, M.; Yu, L.-J.; Kimura, Y.; Madigan, M. T.; Mizoguchi, A.; Humbel, B. M.; Wang-Otomo, Z.-Y. Cryo-EM structure of the photosynthetic LH1-RC complex from *Rhodospirillum rubrum*. *Biochemistry* **2021**, *60*, 2483−2491.
(23) Gardiner, A. T.; Nguyen-Phan, T. C.; Cogdell, R. J. A comparative look at structural variation among RC-LH1 'core' complexes present in anoxygenic phototrophic bacteria. *Photosynth. Res.* **2020**, *145*, 83−96.
(24) Bracun, L.; Yamagata, A.; Christianson, B. M.; Terada, T.; Canniffe, D. P.; Shirouzu, M.; Liu, L.-N. Cryo-EM structure of the photosynthetic RC-LH1-PufX supercomplex at 2.8-Å resolution. *Sci. Adv.* **2021**, *7*, No. eabf8864.
(25) Roszak, A. W.; Howard, T. D.; Southall, J.; Gardiner, A. T.; Law, C. J.; Isaacs, N. W.; Cogdell, R. J. Crystal structure of the RC-LH1 core complex from *Rhodopseudomonas palustris*. *Science* **2003**, *302*, 1969−1972.
(26) Drews, G. Formation of the light-harvesting complex I (B870) of anoxygenic phototrophic purple bacteria. *Arch. Microbiol.* **1996**, *166*, 151−159.
(27) Cogdell, R. J.; Gall, A.; Köhler, J. The architecture and function of the light-harvesting apparatus of purple bacteria: from single molecules to in vivo membranes. *Q. Rev. Biophys.* **2006**, *39*, 227−324.
(28) Ferretti, M.; Duquesne, K.; Strugis, J. N.; van Grondelle, R. Ultrafast excited state processes in *Roseobacter denitrificans* antennae: Comparison of isolated complexes and native membranes. *Phys. Chem. Chem. Phys.* **2014**, *16*, 26059−26066.
(29) Blankenship, R. E. *Molecular Mechanisms of Photosynthesis*; John Wiley & Sons, 2014.
(30) Tan, L.-M.; Yu, J.; Kawakami, T.; Kobayashi, M.; Wang, P.; Wang-Otomo, Z.-Y.; Zhang, Y.-P. New insights into the mechanism of uphill excitation energy transfer from core antenna to reaction center in purple photosynthetic bacteria. *J. Phys. Chem. Lett.* **2018**, *9*, 3278−3284.
(31) Allen, J.; Williams, J. Photosynthetic reaction centers. *FEBS Lett.* **1998**, *438*, 5−9.
(32) Ma, F.; Yu, L.-J.; Wang-Otomo, Z.-Y.; van Grondelle, R. Temperature dependent LH1 →RC energy transfer in purple bacteria *Tch. tepidum* with shiftable LH1-Q_y band: A natural system to investigate thermally activated energy transfer in photosynthesis. *Biochim. Biophys. Acta, Bioenerg.* **2016**, *1857*, 408−414.
(33) Visscher, K. J.; Bergström, H.; Sundström, V.; Hunter, C. N.; van Grondelle, R. Temperature dependence of energy transfer from the long wavelength antenna BChl-896 to the reaction center in *Rhodospirillum rubrum*, *Rhodobacter sphaeroides* (w.t. and M21 mutant) from 77 to 177K, studied by picosecond absorption spectroscopy. *Photosynth. Res.* **1989**, *22*, 211−217.
(34) Permentier, H. P.; Neerken, S.; Schmidt, K. A.; Overmann, J.; Amesz, J. Energy transfer and charge separation in the purple non-sulfur bacterium *Roseospirillum parvum*. *Biochim. Biophys. Acta, Bioenerg.* **2000**, *1460*, 338−345.
(35) Ma, F.; Kimura, Y.; Zhao, X.-H.; Wu, Y.-S.; Wang, P.; Fu, L.-M.; Wang, Z.-Y.; Zhang, J.-P. Excitation dynamics of two spectral forms of the core complexes from photosynthetic bacterium *Thermochromatium tepidum*. *Biophys. J.* **2008**, *95*, 3349−3357.
(36) Beyer, S. R.; Müller, L.; Southall, J.; Cogdell, R. J.; Ullmann, G. M.; Köhler, J. The open, the closed, and the empty: Time-resolved fluorescence spectroscopy and computational analysis of RC-LH1 complexes from *Rhodopseudomonas palustris*. *J. Phys. Chem. B* **2015**, *119*, 1362−1373.
(37) Bernhardt, K.; Trissl, H.-W. Escape probability and trapping mechanism in purple bacteria: Revisited. *Biochim. Biophys. Acta, Bioenerg.* **2000**, *1457*, 1−17.
(38) Timpmann, K.; Zhang, F. G.; Freiberg, A.; Sundström, V. Detrapping of excitation energy from the reaction centre in the photosynthetic purple bacterium *Rhodospirillum rubrum*. *Biochim. Biophys. Acta, Bioenerg.* **1993**, *1183*, 185−193.
(39) Freiberg, A.; Godik, V. I.; Pullerits, T.; Timpman, K. Picosecond dynamics of directed excitation transfer in spectrally heterogeneous light-harvesting antenna of purple bacteria. *Biochim. Biophys. Acta, Bioenerg.* **1989**, *973*, 93−104.
(40) Sundström, V.; van Grondelle, R.; Bergström, H.; Åkesson, E.; Gillbro, T. Excitation-energy transport in the bacteriochlorophyll antenna systems of *Rhodospirillum rubrum* and *Rhodobacter sphaeroides*, studied by low-intensity picosecond absorption spectroscopy. *Biochim. Biophys. Acta, Bioenerg.* **1986**, *851*, 431−446.
(41) Van Grondelle, R.; Bergström, H.; Sundström, V.; Gillbro, T. Energy transfer within the bacteriochlorophyll antenna of purple

https://doi.org/10.1021/jacs.5c12301
J. Am. Chem. Soc. 2025, 147, 36706−36716

bacteria at 77 K, studied by picosecond absorption recovery. *Biochim. Biophys. Acta, Bioenerg.* **1987**, *894*, 313−326.
(42) Denisov, I. G.; Sligar, S. G. Nanodiscs in membrane biochemistry and biophysics. *Chem. Rev.* **2017**, *117*, 4669−4713.
(43) Duquesne, K.; Blanchard, C.; Sturgis, J. N. Molecular origins and consequences of high-800 LH2 in *Roseobacter denitrificans*. *Biochemistry* **2011**, *50*, 6723−6729.
(44) Tang, K.; Zong, R.; Zhang, F.; Xiao, N.; Jiao, N. Characterization of the photosynthetic apparatus and proteome of *Roseobacter denitrificans*. *Curr. Microbiol.* **2010**, *60*, 124−233.
(45) Richter, M. F.; Baier, J.; Cogdell, R. J.; Köhler, J.; Oellerich, S. Single-molecule spectroscopic characterization of light-harvesting 2 complexes reconstituted into model membranes. *Biophys. J.* **2007**, *93*, 183−191.
(46) Pflock, T.; Dezi, M.; Venturoli, G.; Cogdell, R. J.; Köhler, J.; Oellerich, S. Comparison of the fluorescence kinetics of detergent-solubilized and membrane-reconstituted LH2 complexes from *Rps. acidophila and Rb. sphaeroides*. *Photosynth. Res.* **2008**, *95*, 291−298.
(47) Böhm, P. S.; Kunz, R.; Southall, J.; Cogdell, R. J.; Köhler, J. Does the reconstitution of RC-LH1 complexes from *Rhodopseudomonas acidophila* strain 10050 into a phospholipid bilayer yield the optimum environment for optical spectroscopy? *J. Phys. Chem. B* **2013**, *117*, 15004−15013.
(48) Trissl, H. W.; Law, C. J.; Cogdell, R. J. Uphill energy transfer in LH2-containing purple bacteria at room temperature. *Biochim. Biophys. Acta, Bioenerg.* **1999**, *1412*, 149−172.
(49) Crouch, L. I.; Holden-Dye, K.; Jones, M. R. Dimerisation of the *Rhodobacter sphaeroides* RC-LH1 photosynthetic complex is not facilitated by a GxxxG motif in the PufX polypeptide. *Biochim. Biophys. Acta, Bioenerg.* **2010**, *1797*, 1812−1819.
(50) Freiberg, A.; Allen, J. P.; Williams, J. C.; Woodbury, N. W. Energy trapping and detrapping by wild type and mutant reaction centers of purple non-sulfur bacteria. *Photosynth. Res.* **1996**, *48*, 309−319.
(51) Freiberg, A.; Timpmann, K. Picosecond fluorescence spectroscopy of light-harvesting antenna complexes from *Rhodospirillum rubrum* in the 300−4 K temperature range. Comparison with the data on chromatophores. *J. Photochem. Photobiol., B* **1992**, *15*, 151−158.
(52) Sebban, P.; Jolchine, G.; Moya, I. Spectra of fluorescence lifetime and intensity of *Rhodopseudomonas sphaeroides* at room and low temperature. *Photochem. Photobiol.* **1984**, *39*, 247−253.
(53) Scheuring, S.; Seguin, J.; Marco, S.; Lëvy, D.; Robert, B.; Rigaud, J.-L. Nanodissection and high-resolution imaging of the *Rhodopseudomonas viridis* photosynthetic core complex in native membranes by AFM. *Proc. Natl. Acad. Sci. U.S.A.* **2003**, *100*, 1690−1693.
(54) Bahatyrova, S.; Frese, R. N.; van der Werf, K. O.; Otto, C.; Hunter, C. N.; Olsen, J. D. Flexibility and size heterogeneity of the LH1 light harvesting complex revealed by atomic force microscopy: Functional significance for bacterial photosynthesis. *J. Biol. Chem.* **2004**, *279*, 21327−21333.
(55) Wang, D.; Fiebig, O. C.; Harris, D.; Toporik, H.; Ji, Y.; Chuang, C.; Nairat, M.; Tong, A. L.; Ogren, J. I.; Hart, S. M.; Cao, J.; Sturgis, J. N.; Mazor, Y.; Schlau-Cohen, G. S. Elucidating interprotein energy transfer dynamics within the antenna network from purple bacteria. *Proc. Natl. Acad. Sci. U.S.A.* **2023**, *120*, No. e2220477120.
(56) Lu, Y.; Zhang, H.; Niedzwiedzki, D. M.; Jiang, J.; Blankenship, R. E.; Gross, M. L. Fast photochemical oxidation of proteins maps the topology of intrinsic membrane proteins: Light-harvesting complex 2 in a nanodisc. *Anal. Chem.* **2016**, *88*, 8827−8834.
(57) Guarnetti Prandi, I.; Sláma, V.; Pecorilla, C.; Cupellini, L.; Mennucci, B. Structure of the stress-related LHCSR1 complex determined by an integrated computational strategy. *Commun. Biol.* **2022**, *5*, No. 145.
(58) Liguori, N.; Campos, S. R. R.; Baptista, A. M.; Croce, R. Molecular anatomy of plant photoprotective switches: The sensitivity of PsbS to the environment, residue by residue. *J. Phys. Chem. Lett.* **2019**, *10*, 1737−1742.
(59) Liguori, N.; Roy, L. M.; Opacic, M.; Durand, G.; Croce, R. Regulation of light harvesting in the green alga *Chlamydomonas reinhardtii*: The C-terminus of LHCSR is the knob of a dimmer switch. *J. Am. Chem. Soc.* **2013**, *135*, 18339−18342.
(60) van Bezouwen, L. S.; Caffarri, S.; Kale, R. S.; Kouřil, R.; Thunnissen, A.-M. W. H.; Oostergetel, G. T.; Boekema, E. J. Subunit and chlorophyll organization of the plant photosystem II supercomplex. *Nat. Plants* **2017**, *3*, No. 17080.
(61) Gisriel, C. J.; Brudvig, G. W. Comparison of PsbQ and Psb27 in photosystem II provides insight into their roles. *Photosynth. Res.* **2022**, *152*, 177−191.
(62) di Luccio, E.; Koehl, P. A quality metric for homology modeling: The H-factor. *BMC Bioinf.* **2011**, *12*, No. 48.
(63) Nayeem, A.; Sitkoff, D.; Krystek, S., Jr. A comparative study of available software for high-accuracy homology modeling: From sequence alignments to structural models. *Protein Sci.* **2006**, *15*, 808−824.
(64) Forrest, L. R.; Tang, C. L.; Honig, B. On the accuracy of homology modeling and sequence alignment methods applied to membrane proteins. *Biophys. J.* **2006**, *91*, 508−517.
(65) Ma, F.; Yu, L.-J.; Hendrix, R.; Wang-Otomo, Z.-Y.; van Grondelle, R. Direct observation of energy detrapping in LH1-RC complex by two-dimensional electronic spectroscopy. *J. Am. Chem. Soc.* **2017**, *139*, 591−594.
(66) Timpmann, K.; Freiberg, A.; Sundström, V. Energy trapping and detrapping in the photosynthetic bacterium *Rhodopseudomonas viridis*: Transfer-to-trap limited dynamics. *Chem. Phys.* **1995**, *194*, 275−283.
(67) Xiao, W.; Lin, S.; Taguchi, A. K. W.; Woodbury, N. W. Femtosecond pump-probe analysis of energy and electron transfer in photosynthetic membranes of *Rhodobacter capsulatus*. *Biochemistry* **1994**, *33*, 8313−8322.
(68) Fassioli, F.; Olaya-Castro, A.; Scheuring, S.; Sturgis, J. N.; Johnson, N. F. Energy transfer in light-adapted photosynthetic membranes: From active to saturated photosynthesis. *Biophys. J.* **2009**, *97*, 2464−2473.
(69) Şener, M. K.; Olsen, J. D.; Hunter, C. N.; Schulten, K. Atomic-level structural and functional model of a bacterial photosynthetic membrane vesicle. *Proc. Natl. Acad. Sci. U.S.A.* **2007**, *104*, 15723−15728.
(70) Skar-Gislinge, N.; Johansen, N. T.; Høiberg-Nielsen, R.; Arleth, L. Comprehensive study of the self-assembly of phospholipid nanodiscs: What determines their shape and stoichiometry? *Langmuir* **2018**, *34*, 12569−12582.
(71) Sturgis, J. N.; Gall, A.; Ellervee, A.; Freiberg, A.; Robert, B. The effect of pressure on the bacteriochlorophyll a binding sites of the core antenna complex from Rhodospirillum rubrum. *Biochemistry* **1998**, *37*, 14875−14880.
(72) Nogi, T.; Hirano, Y.; Miki, K. Structural and functional studies on the tetraheme cytochrome subunit and its electron donor proteins: The possible docking mechanisms during the electron transfer reaction. *Photosynth. Res.* **2005**, *85*, 87−99.
(73) Bracun, L.; Yamagata, A.; Christianson, B. M.; Shirouzu, M.; Liu, L.-N. Cryo-EM structure of a monomeric RC-LH1-PufX supercomplex with high-carotenoid content from *Rhodobacter capsulatus*. *Structure* **2023**, *31*, 318−328.
(74) Tani, K.; Kanno, R.; Ji, X.-C.; Satoh, I.; Y, K.; Hall, M.; Yu, L.-J.; Kimura, Y.; Mizoguchi, A.; Humbel, B. M.; Madigan, M. T.; Wang-Otomo, Z.-Y. *Rhodobacter capsulatus* forms a compact crescent-shaped LH1-RC photocomplex. *Nat. Commun.* **2023**, *14*, No. 846.
(75) Tani, K.; Nagashima, K. V. P.; Kanno, R.; Kawamura, S.; Kikuchi, R.; Hall, M.; Yu, L.-J.; Kimura, Y.; Madigan, M. T.; Mizoguchi, A.; Humbel, B. N.; Wang-Otomo, Z.-Y. A previously unrecognized membrane protein in the *Rhodobacter sphaeroides* LH1-RC photocomplex. *Nat. Commun.* **2021**, *12*, No. 6300.
(76) Qian, P.; Swainsbury, D. J. K.; Croll, T. I.; Salisbury, J. H.; Martin, E. C.; Jackson, P. J.; Hitchcock, A.; Castro-Hartmann, P.; Sader, K.; Hunter, C. N. Cryo-EM structure of the monomeric

https://doi.org/10.1021/jacs.5c12301
J. Am. Chem. Soc. 2025, 147, 36706−36716

Rhodobacter sphaeroides RC-LH1 core complex at 2.5 Å. *Biochem. J.* **2021**, *478*, 3775−3790.
(77) Qian, P.; Croll, T. I.; Hitchcock, A.; Jackson, P. J.; Salisbury, J. H.; Castro-Hartmann, P.; Sader, K.; Swainsbury, D. J. K.; Hunter, C. N. Cryo-EM structure of the dimeric *Rhodobacter sphaeroides* RC-LH1 core complex at 2.9 Å: The structural basis for dimerisation. *Biochem. J.* **2021**, *478*, 3923−3937.
(78) Qian, P.; Papiz, M. Z.; Jackson, P. J.; Brindley, A. A.; Ng, I. W.; Olsen, J. D.; Dickman, M. J.; Bullough, P. A.; Hunter, C. N. Three-dimensional structure of the *Rhodobacter sphaeroides* RC-LH1-PufX complex: Dimerization and quinone channels promoted by PufX. *Biochemistry* **2013**, *52*, 7575−7585.
(79) Cao, P.; Bracun, L.; Yamagata, A.; Christianson, B. M.; Negami, T.; Zou, B.; Terada, T.; Canniffe, D. P.; Shirouzu, M.; Li, M.; Liu, L.-N. Structural basis for the assembly and quinone transport mechanisms of the dimeric photosynthetic RC-LH1 supercomplex. *Nat. Commun.* **2022**, *13*, No. 1977.
(80) Swingley, W. D.; Sadekar, S.; Mastrian, S. D.; et al. The complete genome sequence of *Roseobacter denitrificans* reveals a mixotrophic rather than photosynthetic metabolism. *J. Bacteriol.* **2007**, *189*, 683−690.
(81) Tani, K.; Kanno, R.; Kurosawa, K.; Takaichi, S.; Nagashima, K. V. P.; Hall, M.; Yu, L.-J.; Kimura, Y.; Madigan, M. T.; Mizoguchi, A.; Humbel, B. M.; Wang-Otomo, Z.-Y. An LH1-RC photocomplex from an extremophilic phototroph provides insight into origins of two photosynthesis proteins. *Commun. Biol.* **2022**, *5*, No. 1197.
(82) Kishi, R.; Imanishim, M.; Kobayashi, M.; Takenaka, S.; Madigan, M. T.; Wang-Otomo, Z. Y.; Kimura, Y. Quinone transport in the closed light-harvesting 1 reaction center complex from the thermophilic purple bacterium *Thermochromatium tepidum*. *Biochim. Biophys. Acta, Bioenerg.* **2021**, *1862*, No. 148307.
(83) Mao, R.; Guo, J.; Bie, L.; Liu, L.-N.; Gao, J. Tunneling mechanisms of quinones in photosynthetic Reaction Center-Light Harvesting 1 supercomplexes. *Small Sci.* **2024**, *4*, No. 2400188.
(84) Rinyu, L.; Martin, E. W.; Takahashi, E.; Maróti, P.; Wraight, C. A. Modulation of the free energy of the primary quinone acceptor (Q_A) in reaction centers from *Rhodobacter sphaeroides*: Contributions from the protein and protein-lipid (cardiolipin) interactions. *Biochim. Biophys. Acta, Bioenerg.* **2004**, *1655*, 93−101.
(85) Fiebig, O. C. Understanding Ultrafast Energy Transfer across the Photosynthetic Membrane of Purple Bacteria with Near-Native Systems. Ph.D. Thesis, Massachusetts Institute of Technology: Cambridge, MA, 2022.

https://doi.org/10.1021/jacs.5c12301
J. Am. Chem. Soc. 2025, 147, 36706−36716